J. Math. Biol.
DOI 10.1007/s00285-016-0984-6

become variable. This is because the rise and decay of the adaptation variable is now stochastically-driven, leading to a distribution of transition times. Interestingly, common noise in the adaptation variable can lead to a correlation of two distinct slow oscillating populations. This effect is still significant in the event that each population

tions between the quiescent and active state (Parga and Abbott 2007; Bressloff 2010; Litwin-Kumar and Doiron 2012). Alternatively, switches between low and high activity states may arise by some underlying systematic slow process. For instance, it has been shown that competition between recurrent excitation and the negative feedback produced by activity-dependent synaptic depression can lead to slow oscillations in firing rate whose timescale is set by the depression timescale (Bart et al. 2005; Holcman and Tsodyks 2006; Kilpatrick and Bressloff 2010). Excitatory-inhibitory networks with facilitation can produce slow oscillations, due to the slow facilitation of feedback inhibition that terminates the up state, the down state is then rekindled due to positive feedback from recurrent excitation (Melamed et al. 2008). These neural mechanisms utilize dynamic changes in the strength of neural architecture. However, Compte et al. (2003) proposed that single cell mechanisms can also shift network states between up and down states. The up state is maintained by strong recurrent excitation balanced by inhibition, and transitions to the down state occur due to a slow hyperpolarizing current. Once in the down state, the slow hyperpolarizing current is inactivated, and excitation reinitiates the up state. Slow hyperpolarizing currents are prime examples of mechanisms underlying spike rate adaptation (Benda and Herz 2003). One particularly

While the synchronous initiation of up states may be explained by recurrent architecture, synchronization of the down states are more difficult to explain and remain an unexplained phenomenon (Volgushev et al. 2006). The fact that the onset of quiescence is fast and well synchronized means there must be either a rapid relay signal between all foci or there is some global signal cueing the down state. Rather than suggest a disynaptic relay, using long range excitation acting on local inhibition, we suggest that background noise can serve as a synchronizing global signal (Ermentrout et al. 2008). For example, up/down state correlations in visual cortex have also been observed across 500 μm, and it has been suggested this may arise due to common input from LGN (Lampl et al. 1999). Noisy but correlated inputs have been shown to be capable of synchronizing uncoupled populations of phase oscillators (Teramae and Tanaka 2004) as well as experimentally recorded cells in vitro (Galán et al. 2006). Here we will show correlated noise is a viable mechanisms for coordinating slow oscillations in distinct uncoupled neural populations.

The paper is organized as follows: We introduce the neural population model in Sect. 2, indicating the way external noise is incorporated into the model. In Sect. 3, we demonstrate the periodic solutions that emerge in the noise-free model, demonstrating it is possible to derive analytical expressions for the oscillation period in the case of steep firing rate functions. Then, in Sect. 4 we show how to derive phase sensitivity functions that describe how external perturbations to the periodic solution impact the asymptotic phase of the oscillation. As demonstrated, the impact of perturbations to the adaptation variable is much stronger than activity variable perturbations, especially for longer adaptation timescales. Thus, our studies of the impact of noise mainly focus on the effects of fluctuations in the adaptation variable. We find, in Sect. 5, that adding noise to the adaptation variable leads to up and down state durations that are shorter and more balanced, so that the up and down state last for similar lengths of time. In Sect. 6, we demonstrate that slow oscillations in distinct populations can become entrained to one another when both populations are forced by the same common noise signal. This phenomenon is robust to the introduction of independent noise in each population, as we show in Sect. 7. Lastly, we demonstrate that the rate and spike patterns of two uncoupled spiking networks can be synchronized by common noise in Sect. 8.

2 Adaptive neural populations: deterministic and stochastic models

We begin by describing the models we will use to explore the impact of external perturbations on slow oscillations. Motivated by Compte et al. (2003), we will focus on a neural population model with spike rate adaptation, akin to mutual inhibitory models

Here, represents the mean firing rate of the neural population with excitatory connection strength α. The negative feedback variable ⁄ is spike frequency adaptation with strength ϕ and time constant τ. For some of our analysis we will utilize the assumption $\tau \gg 1$, based on the fact that many forms of spike rate adaptation tend to be much slower than neural membrane time constants (Benda and Herz 2003). The constant tonic drive initiates the high firing rate (up) state, and slow adaptation eventually attenuates activity to a low firing rate (down) state. Weak but positive drive 0 is meant to model the presence of low spiking threshold cells that spontaneously fire, utilized as a mechanism for initiating the up state in Compte et al. (2003). The firing rate function , is monotone and saturating function such as the sigmoid

$$= \frac{1}{1 + \mathrm{e}^{-\gamma}} \tag{2}$$

Commonly, in studies of neural field models, the high gain limit ($\gamma \to \infty$) of Eq. (2) is taken to yield the Heaviside firing rate function (Amari 1977; Laing and Chow 2002)

$$= \begin{cases} 1: & \geq 0 \\ 0: & 0 \end{cases} \tag{3}$$

which often allows for a more straightforward analytical study of model dynamics. We exploit this fact extensively in our study. Nonetheless, we have also carried out many numerical simulations of the model for a smooth firing rate function Eq. (2), and they correspond to the results we present for sufficiently high gain. Note, this form of adaptation is often referred to as ⁄ , negative feedback, as current is subtracted from the population input. Alternative models of slow neural population

$\langle \xi_{\checkmark}{}^{2} \rangle = \sigma_{\checkmark}^{2}$. Extending our results concerning the phase response curve, we will explore how noise forcing impacts the statistics of the resulting stochastic oscillations in Eq. (4). In particular, since we find noise tends to impact the phase of the oscillation more strongly when applied to the adaptation variable, we will tend to focus on the case $\xi \equiv 0$.

Stochastic dual population model Finally, we will focus on how correlations in noise-forcing impact the coherence of two distinct uncoupled populations

$$\mathrm{d}_{1} = [-_{1} + , \alpha_{1} -\checkmark_{1} +]\mathrm{d} + \mathrm{d}\xi \tag{5a}$$

$$\mathrm{d}\checkmark_{1} = [-\checkmark_{1} + \phi_{1}]\mathrm{d} \tau + \mathrm{d}\xi_{\checkmark} \tag{5b}$$

$$\mathrm{d}_{2}$$

Fig. 1

Since ¯ is monotone increasing, then ¯ −ˏ ¯ is monotone increasing. Further, noting $\lim_{\text{-}\to\pm\infty}[\bar{}-\text{ˏ}\ \bar{}\ ] = \pm\infty$, it is clear ¯ −ˏ ¯ crosses zero once, so Eq. (7) has a single root when $\phi\quad\alpha$. Stability of this equilibrium is given by the eigenvalues of the associated Jacobian

$$\bar{}\,\text{ˊ}\ =$$

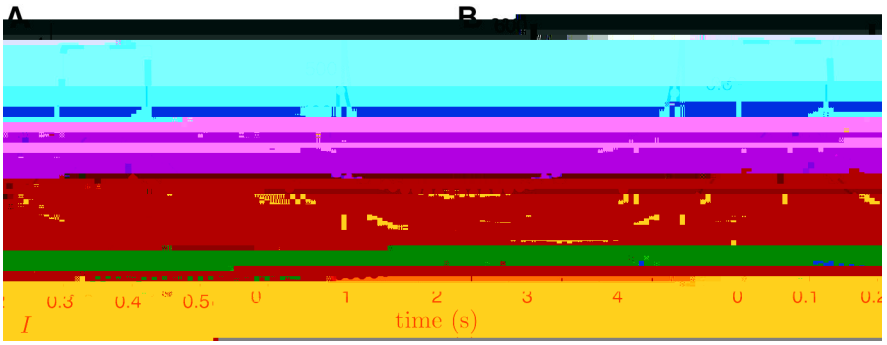

Fig. 2

$_1$ of the adaptation variable a increases monotonically with input

$$\frac{\mathrm{d}\ _1}{\mathrm{d}} = \frac{\tau\alpha}{\phi - \quad \phi - \alpha -} \quad 0$$

when 0 $\phi - \alpha$. Furthermore, the decay time $_2$ of the adaptation variable a decreases monotonically with input

$$\frac{\mathrm{d}\ _2}{\mathrm{d}} = -\frac{\tau\alpha}{+\alpha} \quad 0$$

when 0 $\phi - \alpha$. Thus, as $\to 0^+$, the slow oscillation's period is dominated by very long decay times $_2 \gg 1$ and as $\to \phi - \alpha\ ^-$, it is dominated by very long rise times $_1 \gg 1$. We can identify the minimal period as a function of the input by finding the critical point of . To do so, we differentiate and simplify

$$\frac{\mathrm{d}}{\mathrm{d}} = -\frac{\tau\alpha\phi\ 2\ - \ \phi - \alpha}{+\alpha\ \ \phi - \quad \phi - \alpha -}$$

so the critical point of is at $= \phi - \alpha\ \ 2$, which corresponds to the minimal value of the period $= 2\tau \ln[\ \phi + \alpha \quad \phi - \alpha\ ]$ as pictured in Fig. 2b.

4 Phase response curves

We can further understand the dynamics of the slow oscillations in Eq. (1) by computing phase response curves for both the case of a sigmoidal firing rate Eq. (2) and the Heaviside firing rate Eq. (3). As we will show, perturbations of the activity variable have decreasing impact as the timescale of adaptation τ and the gain γ of the firing

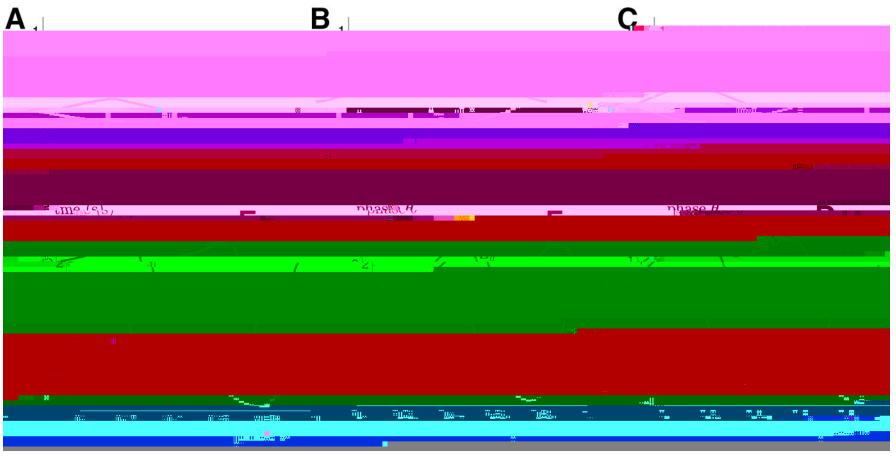

Fig. 3 **a**, **b**, **c** Periodic solution ′ and **d**, **e**, **f** phase sensitivity function ′ of Eq. (1) plotted as a function of phase $\theta =$ for a sigmoidal firing rate function Eq. (2). **a**, **d** For shorter adaptation timescale $\tau = 10$ and input $= 0\ 2$, the activity variable has a more rounded trajectory, so perturbations to activity

phase advance and phase delay region of the adaptation phase response (′) for larger timescales τ.

In addition to a general formula for the phase sensitivity functions ′ , we can derive an amplitude-dependent formula for the response of limit cycle solutions 0 ′0 of Eq. (1) with a Heaviside firing rate Eq. (3), assuming $\tau \gg 1$. In this case, we utilize the formula for the period Eq. (14) and limit cycle Eq. (15), derived using a separation of timescales assumption. Then, we can compute the change to the variables ′ as a result of a perturbation δ δ′ , which we denote 0 ′0 $\overset{\delta\ \delta'}{\longmapsto}$ ˜0 ˜′0 . We are primarily interested in how the relative time in the limit cycle is altered by a perturbation δ - how much closer or further the limit cycle is to the end of the period after being perturbed. We can readily determine this by first inverting the formula we have for 0 ′0 , given by Eq. (15), to see how this value determines the time 0 along the limit cycle

$$0 \quad 0\,'0 = \begin{cases} \tau \ln[\ \phi - \quad \phi - '0\ ] : \ 0 = 1 \\ \tau \ln[\ \phi - \quad + \alpha\ '0\ \ \phi - \alpha - \ ] : \ 0 = 0 \end{cases} \tag{18}$$

Using this formula, we can now map the value ˜0 ˜′0 to an associated updated relative time 0 along the oscillation.

Here, we decompose the impact of perturbations to the and′ variables. We begin by studying the impact of perturbations δ to the activity variable . We can directly compute

$$\tilde{}0 \quad = \quad + \alpha[\ 0 \quad + \delta\ ] - '0$$

Thus, the singular system Eq. (13) will be unaffected by such perturbations if sgn $+$ $\alpha[\ +\delta\ ] - ' = \text{sgn}\ +\alpha\ -'$. This is related to the flatness of the susceptibility function over much of the time domain in Fig. 3d–f. However, if sgn $+\alpha[\ +$ $\delta\ ] - ' \neq \text{sgn}\ +\alpha\ -'$, then ˜0 $= 1 -$ 0 , as detailed in the following piecewise smooth map:

$$\begin{array}{llllll} 0 & = 0 \mapsto \tilde{}0 & = 1 & : \delta & - & -'0 \quad \alpha \quad 0 \\ 0 & = 0 \mapsto \tilde{}0 & = 0 & : \delta & - & -'0 \quad \alpha \quad 0 \end{array}$$

Fig. 4 Phase response curves of the fast–slow timescale separated system $\tau \gg 1$. **a**, **b** Amplitude δ- and $\delta_{\prime}$-dependent phase response curves $\theta\ \delta$ and $_{\prime}\ \theta\ \delta$ characterizing phase advances/delays resulting from perturbation of neural activity and adaptation $\prime$. We compare analytical formulae ( ) to numerically computed PRCs ($\prime$). **c**

so $\tilde{}_0 = \quad -$ with $= \tau \ln [\nearrow_0 + \delta_0$], but if $\nearrow_0 \quad + \delta_\nearrow$, so that it is necessary that $\delta_\nearrow \quad 0$, then

$$\tilde{}_0 \quad = 1 \quad \tilde{\nearrow}_0 \quad = \quad + \alpha \ \mathrm{e}^{- \ - 1 \ \tau} + \delta_\nearrow \tag{23}$$

In the case of Eq. (

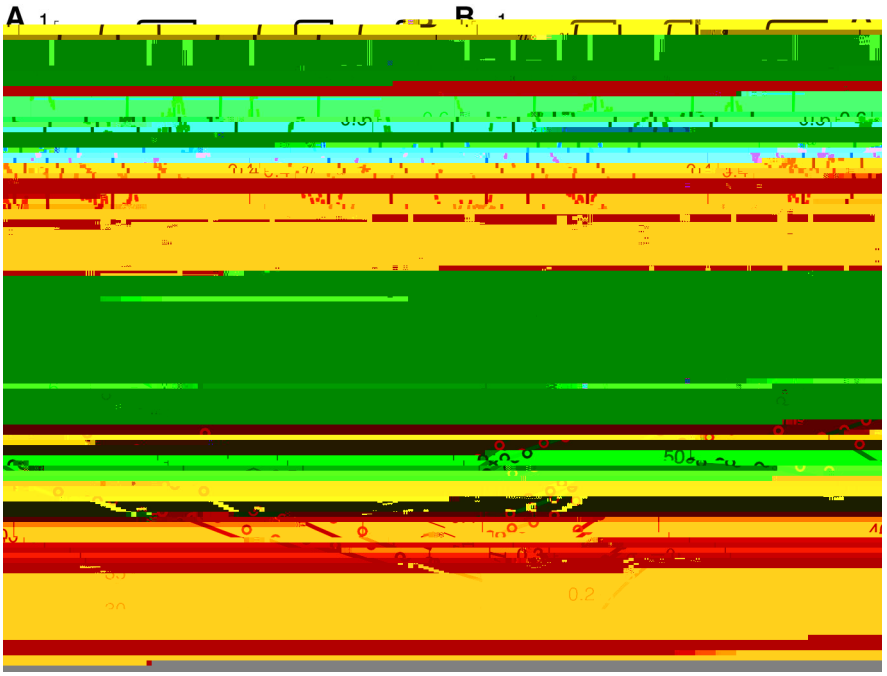

Fig. 5 Noise alters the duration of up and down states. **a** Numerical simulation of the stochastically driven population model Eq. (4) demonstrates up and down state durations (e.g., $_1$ and $_2$) are variable when driven by adaption noise $\xi_{\prime}$ with $\langle \xi_{\prime}^2 \rangle = \sigma_{\prime}^2$, $\sigma_{\prime} = 0\ 01$. Switches are determined by the threshold crossings of the adaptation variable $_{\prime} =$ and $_{\prime} = +\alpha$. **b** Up/down states become more variable when the noise amplitude $\sigma_{\prime} = 0\ 02$. **c** Mean durations of the up and down state, $\langle\ _1\rangle$ and $\langle\ _2\rangle$, decrease as a function noise amplitude $\sigma_{\prime}$. **d** Impact of noise $\sigma_{\prime}$ on the balance of up to down state durations $\bar{}_1\ \bar{}_2$ as input is varied. Firing rate is given by the Heaviside function Eq. (3). Other parameters are $\alpha = 0\ 5$, $\phi = 1$, and $\tau = 50$

which is the well-known threshold crossing problem for an Ornstein-Uhlenbeck process (Gardiner 2004). The mean $\bar{}_1$ of the passage time distribution is thus given by defining the potential $_{\prime} = \frac{\prime^2}{2\tau} - \frac{\phi_{\prime}}{\tau}$ and computing the integral

$$\bar{}_1 = \frac{1}{\sigma_{\prime}^2} \int_{-\infty}^{+\alpha} e^{[}$$

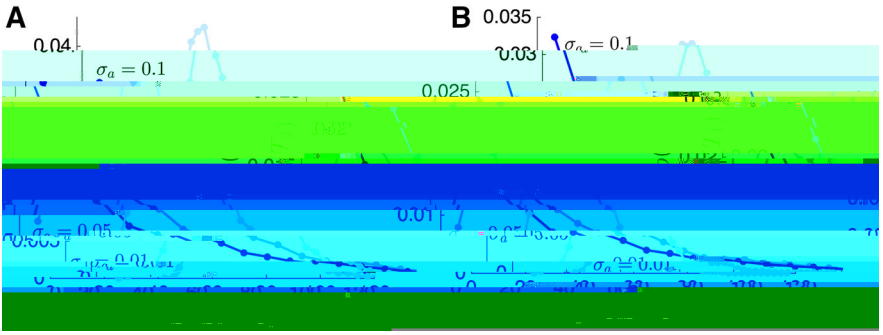

Fig. 6 Noise reshapes the distributions of (**a**) up and (**b**) down state durations. As the level of noise $\sigma_{\prime}$ is increased, the intrinsic period of the deterministic oscillation is masked by the predominance of durations punctuated by noise-driven transitions. This results in an exponentially decaying distribution, rather than a peaked distribution, for large noise levels $\sigma_{\prime}$. Firing rate is given by the Heaviside function Eq. (3). Other parameters are $= 0\ 2$, $\alpha = 0\ 5$, $\phi = 1$, and $\tau = 50$

experimental papers exploring the statistics of up and down states (Isomura et al. 2006; Sanchez-Vives and McCormick 2000; Steriade et al. 1993; Cunningham et al. 2006).

6 Synchronizing two uncoupled populations

Now, we demonstrate that common noise can synchronize the up and down states of two distinct and uncoupled populations. We begin with the case of identical noise and then, in Sect. 7, relax these assumptions to show that some level of coherence is still possible when each population has an intrinsic and an independent source of noise. This is motivated by the observation that the SDE derived in the large system-size limit of a neural master equation tends to possess intrinsic noise in each population, in addition to an extrinsic common noise term (Bressloff and Lai 2011). As we will show, intrinsicAs)..0-283.2000001(in)-2disrupt3.20001(term)-217.39/Cs6Tc [()pha)o[3/Cs6Tc [(

Fig. 8 Slow oscillations in Eq. (5) can also be synchronized via common noise to the neural activity variables ($\langle \xi^2 \rangle = \quad ^2$). Lyapunov exponent λ decreases as a function of the adaptation timescale τ, for $\quad = 0$

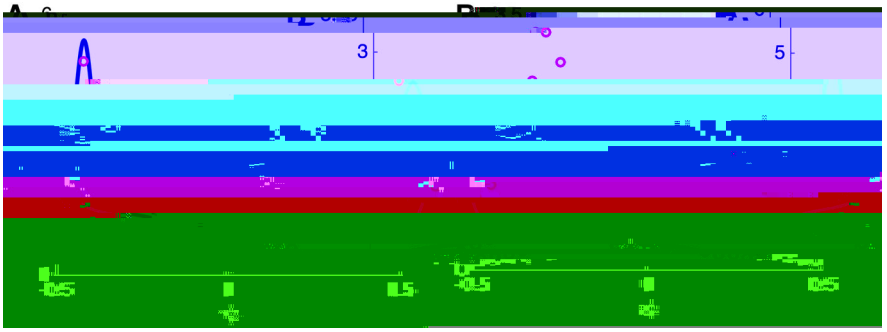

Fig. 9 Stationary density $_0$ of the phase difference $= \theta_1 - \theta_2$ for two slowly oscillating neural population driven by both common and independent noise Eq. (6). As the degree of noise correlation is decreased from (**a**) $\chi_{\prime} = 0\ 95$ to (**b**) $\chi_{\prime} = 0\ 90$, the density spreads, but there is still a peak at $= 0$, the phase-locked state. We focus on noise in the adaptation variable, so $\sigma = 0$ and $\sigma_{\prime} = 0\ 01$. Other parameters are $\alpha = 0\ 5$, $\gamma = 15$, $\phi = 1$, and $\tau = 20$

each of the neural populations. We demonstrate here that oscillation phases of stochastically driven populations still remain relatively close in this case (Fig. 9). Independent noise is incorporated into the modified model Eq. (6). Since there is a periodic solution to the noise-free version of this system, phase-reduction methods can be used to obtain approximate SDEs for the phase variables (Nakao et al. 2007)

$$\mathrm{d}\theta_1 = \omega \mathrm{d} + \mathbf{Z}\ \theta_1 \quad \cdot \mathrm{d}\boldsymbol{\xi} \quad + \mathrm{d}\boldsymbol{\xi}_1 \tag{32a}$$

$$\mathrm{d}\theta_2 = \omega \mathrm{d} + \mathbf{Z}\ \theta_2 \quad \cdot \mathrm{d}\boldsymbol{\xi} \quad + \mathrm{d}\boldsymbol{\xi}$$

Fig. 10 Slow oscillations in an excitatory-inhibitory spiking network of $= 80$ excitatory cells and $= 20$ inhibitory cells. **a** The voltage of two randomly selected excitatory cells shows that periods of quiescence and activity alternate synchronously. **b** Up and down state transitions are apparent in the spike raster plot of all the excitatory cells. **c** Average spike rates of the excitatory populations similarly show the slow switching between the two stable states of the system: a low and a high firing rate state. Parameters are $= 1\,05$, $= 0\,95$, $= 0\,8$ τ , $\tau = 40$ ms, $\tau = 30$ ms, $\tau = 500$ ms, $= 0\,4$, $= 0\,32$, $= 0\,15$, $= 0\,01$, $\sigma = \sigma = \sigma = 0\,01$. Numerical simulations of Eq. (34) employ the Euler–Maruyama method with a timestep $= 10^{-6}$ s

where is the connectivity matrix, τ is the decay time constant of the synapses from population , is the th spike time of neuron in population . Note that excitatory couplings and are non-negative and inhibitory couplings and are non-positive. Lastly, both cell voltage and hyperpolarizing currents are subject to white noise processes ξ with zero mean and variance $\langle \xi \rangle = \sigma^2$ for $= \{ \}$.

The recurrent excitatory connectivity of Eq. (34) generates a bistable network. Sufficiently high spike rates will be sustained, due to repeated reactivation of excitatory cells, but low spike rates do not engender persistent high spike rates. Transitions between these two states are generated by the slow build up and decay of the slow hyperpolarizing currents of the excitatory cells. We demonstrate the ability of the network Eq. (34) to generate synchronous up and down state transitions in Fig. 10. Single cells tend to occupy either a depolarized or hyperpolarized state, where they spike repeatedly or are quiescent (Fig. 10

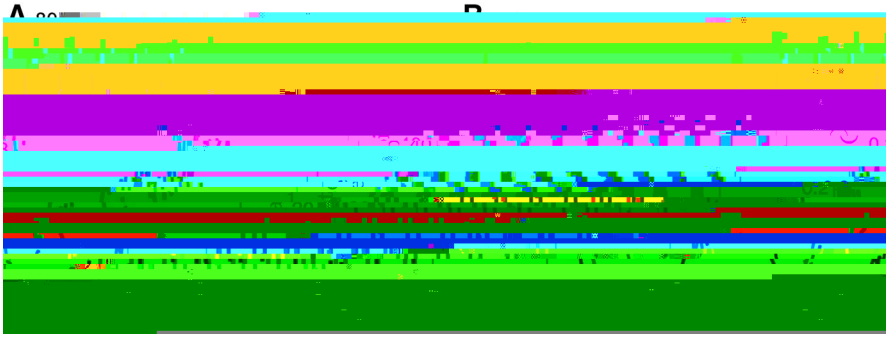

Fig. 11 Noise-induced correlation of the spike pattern of two uncoupled excitatory-inhibitory networks Eq. (34) with adaptation. Noise to all adaptation variables $\sigma = 0.001$ in both populations is fully correlated. **a** Excitatory population-wide spike rates of the first ( ) and second ( ) networks become more correlated over time. Up and down transitions begin to occur more coherently at later times. **b** Correlation coefficient (CC) associated with the spike trains of network 1 as compared to those of network 2, averaged across all possible pairings. The CC for the later time window [3 6]s ( ) is larger than that for the earlier time window [0 3]s ( ), demonstrating the noise-induced increase in activity correlation between the two uncoupled networks. Other parameters and methods are the same as in Fig. 10

Each network's state is initialized randomly, by selecting a random time point in the simulation presented in Fig. 10, so that both networks are in a randomly chosen phase of an evolving slow oscillation. Noise to the voltage variables of each network is taken to be uncorrelated, but noise to the adaptation variables is taken to be fully correlated so that each variable receives an identical white noise sample. As a result, the spike and rate patterns of these two uncoupled networks become more correlated over time (Fig. 11a). We quantify the effect on spike correlation by digitizing all spike times of each network's excitatory population into 10ms bins and then use MATLAB's `xcorr` function to compute an unnormalized correlation function between network 1 and network 2. This is then normalized by dividing by the geometric mean $\sqrt{\quad}$ of both neuron's total firing rate and over the time interval. The time interval [0 3]s is compared to [3 6]s in Fig. 11b, demonstrating the correlation coefficient increases at later times. Thus, common noise in the slow hyperpolarizing currents can help to correlate the temporal evolution of firing rate and spiking in this spiking network model.

9 Discussion

We have studied the impact of deterministic and stochastic perturbations to a neural population model of slow oscillations. The model was comprised of a single recurrently coupled excitatory population with negative feedback from a slow adaptive current (Laing and Chow 2002; Jayasuriya and Kilpatrick 2012). By examining the phase sensitivity function , we found that perturbations of the adaptation variable lead to much larger changes in oscillation phase than perturbations of neural activity. Furthermore, this effect becomes more pronounced as the timescale τ of adaptation is increased. Introducing noise in the model decreases the oscillation period and

helps to balance the mean duration of the oscillation's up and down states. When two uncoupled populations receive common noise, their oscillation phases θ_1 and θ_2 eventually become synchronized, which can be shown by deriving a formula for the Lyapunov exponent of the absorbing state $\theta_1 \equiv \theta_2$ (Teramae and Tanaka 2004). When independent noise is introduced to each population, in addition to common noise, the long-term state of the system is described by a probability density for $\quad = \theta_1 - \theta_2$, which peaks at $\quad \equiv 0$.

Our study was motivated by the observation that recurrent cortical networks can spontaneously generate stochastic oscillations between up and down states. Guided by previous work in spiking models (Compte et al. 2003), we explored a rate model of a recurrent excitatory network with slow spike frequency adaptation. We expect that we would have obtained similar results from an excitatory-inhibitory network, since inhibition tends to act faster than excitation, essentially reducing the effective recurrent excitatory strength (Pinto and Ermentrout 2001). One of the open questions about up and down state transitions concerns the degree to which they are generated by noise or by more deterministic mechanisms, such as slow currents or short term plasticity (Cossart et al. 2003). Here, we have provided some characteristic features that emerge as the level of noise responsible for transitions is increased. Similar questions have been explored in the context of models of perceptual rivalry (Moreno-Bote et al. 2007). In addition, we have provided a plausible mechanism whereby the onset of up and down states could be synchronized in distinct networks (Volgushev et al. 2006).

Nonmonotonic residence time distributions for up states provide compelling evidence for the theory that switches from up to down states are partially governed by deterministic neural processes (Cheng-yu et al. 2009). This idea is explored in detail in a recent study which employed a neuronal network model with short term depression (Dao Duc et al. 2015). Recordings presented therein from both auditory and barrel cortices revealed up state duration distributions which are peaked away from zero. Furthermore, the tail of the duration distribution has an oscillatory decay with several peaks, which may arise due to specific properties of the underlying network's dynamics. Indeed, the authors were able to account for these peaks in a neuronal network model with an up state whose attracting trajectories are oscillatory. It would interesting to extend the present study to try and understand how external inputs might entrain such up and down state transitions that occur via more complex dynamics.

Synchronizing up and down states across multiple areas of the brain may be particularly important for memory consolidation processes (Diekelmann and Born 2010). Long term potentiation (LTP), the process by which the strength of synapses is strengthened for a lasting period of time (Alberini 2009), is one of the chief mechanisms thought to underlie memory formation (Takeuchi et al. 2014). Both cortical and hippocampal LTP are typically restricted to the up states of slow oscillations during slow wave sleep (Rosanova and Ulrich 2005). Furthermore, up states may then repetitively activate memory traces in hippocampus, along with thalamus and cortex, reenforcing memory persistence (Marshall and Born 2007). Thus, subnetworks whose slow oscillations are coordinated are more likely to be further linked through long term plasticity. Indeed, boosting slow oscillations by external potential fields has been shown to enhance declarative memories, providing further evidence that coherent up and down state transitions may subserve memory consolidation processes (Mar-

shall et al. 2006). In total, synchrony may provide a functionally relevant way to link the activities of related neuronal assemblies, allowing appropriate reactivation during waking hours (Steriade 2006).

We have proposed two possible ways for synchrony of up and down states to occur: (a) common noise in the activating currents of neurons in distinct populations and (b) common noise in the slow hyperpolarizing currents of distinct neural populations. The first mechanisms could arise through common excitatory input to each population, as in previous studies of correlation-induced synchrony in olfactory bulb neurons (Galán et al. 2006). The second mechanism must arise via common chemical forcing of hyperpolarizing current. One way this could occur is via common astrocytic calcium signaling (Volterra et al. 2014). Calcium propagates rapidly in waves through astrocytes (Newman 2001), which could generate a common signal on calcium activating hyperpolarizing currents (Bond et al. 2004). Furthermore, slow afterhyperpolarizing currents can be modulated by acetylcholine (Faber and Sah 2005). Global modulations of acetylcholine are often observed during slow wave sleep (Steriade 2004), so this may provide another mechanism for the common perturbation of slow afterhyperpolarizing currents.

Other previous studies have explored phenomenological models of up/down state transitions in neural populations. For instance, Holcman and Tsodyks (2006) intro-

(2009). Interestingly, shared noise can actually stabilize the anti-phase locked state in this case, even though it is unstable in the absence of noise. Furthermore, it is known that coupling spanning long distances can be subject to axonal delays. In spite of this, networks of distantly coupled clusters of cells can still sustain zero-lag synchronized states (Vicente et al. 2008). However, there are some cases in which such delays can destabilize the phase-locked states (Earl and Strogatz 2003; Ermentrout and Ko 2009), in which can another mechanism would be needed to explain the synchronization of up/down states. Thus, we could also explore the impact of delayed coupling, determining how features of phase sensitivity function interact with delay to promote in-phase or anti-phase synchronized states. Lastly, we note that a systematic analysis of phase equations for relaxation oscillators has been applied to the general case of slow variables in (Izhikevich 2000). We expect that the approach developed therein, using the Malkin theorem, could be be applied to the system Eq. (1), even in the case of a discontinuous firing rate function.

References

Ahmed B, Anderson J, Douglas R, Martin K, Whitteridge D (1998) Estimates of the net excitatory currents evoked by visual stimulation of identified neurons in cat visual cortex. Cereb Cortex 8:462–476

Alberini C (2009) Transcription factors in long-term memory and synaptic plasticity. Physiol Rev 89:121–145

Amari S (1977) Dynamics of pattern formation in lateral-inhibition type neural fields. Biol Cybern 27:77–87

Amit DJ, Brunel N (1997) Model of global spontaneous activity and local structured activity during delay periods in the cerebral cortex. Cereb Cortex 7:237–252

Bart E, Bao S, Holcman D (2005) Modeling the spontaneous activity of the auditory cortex. J Comput Neurosci 19:357–378

Benda J, Herz AVM (2003) A universal model for spike-frequency adaptation. Neural Comput 15:2523–2564

Bond CT, Herson PS, Strassmaier T, Hammond R, Stackman R, Maylie J, Adelman JP (2004) Small conductance $ca^{2}+$

Dao Duc K, Parutto P, Chen X, Epsztein J, Konnerth A, Holcman D (2015) Synaptic dynamics and neuronal network connectivity are reflected in the distribution of times in up states. Front Comput Neurosci 9:96

Diekelmann S, Born J (2010) The memory function of sleep. Nat Rev Neurosci 11:114–126

Earl MG, Strogatz SH (2003) Synchronization in oscillator networks with delayed coupling: a stability criterion. Phys Rev E 67:036204

Ermentrout B (1996) Type i membranes, phase resetting curves, and synchrony. Neural Comput 8:979–1001

Ermentrout B, Ko TW (2009) Delays and weakly coupled neuronal oscillators. Philos Trans R Soc Lond A Math Phys Eng Sci 367:1097–1115

Ermentrout GB (2009) Stochastic methods in neuroscience, chapter Noisy Oscillators. Oxford Univ Press, Oxford

Ermentrout GB, Galán RF, Urban NN (2008) Reliability, synchrony and noise. Trends Neurosci 31:428–434

Faber E, Sah P (2005) Independent roles of calcium and voltage-dependent potassium currents in controlling spike frequency adaptation in lateral amygdala pyramidal neurons. Eur J Neurosci 22:1627–1635

Fox MD, Raichle ME (2007) Spontaneous fluctuations in brain activity observed with functional magnetic resonance imaging. Nat Rev Neurosci 8:700–711

Fröhlich F, McCormick DA (2010) Endogenous electric fields may guide neocortical network activity. Neuron 67:129–143

Galán RF, Fourcaud-Trocmé N, Ermentrout GB, Urban NN (2006) Correlation-induced synchronization of oscillations in olfactory bulb neurons. J Neurosci 26:3646–3655

Gardiner CW (2004) Handbook of stochastic methods for physics, chemistry, and the natural sciences. Springer, Berlin

Higgs MH, Slee SJ, Spain WJ (2006) Diversity of gain modulation by noise in neocortical neurons: regulation by the slow afterhyperpolarization conductance. J Neurosci 26:8787–8799

Holcman D, Tsodyks M (2006) The emergence of up and down states in cortical networks. PLoS Comput Biol 2:e23–e23

Isomura Y, Sirota A, Ozen S, Montgomery S, Mizuseki K, Henze DA, Buzsáki G (2006) Integration and